Assessment of Vibrational Non-Equilibrium Effect on Detonation Cell Size

SHI Lisong[1], SHEN Hua[1], ZHANG Peng[1], ZHANG Deliang[2], WEN Chihyung[1,*]

1. Department of Mechanical Engineering, The Hong Kong Polytechnic University, Hong Kong

2. State Key Laboratory of High Temperature Gas Dynamics, Institute of Mechanics, Chinese Academy of Sciences, China

*Corresponding author, E-mail: cywen@polyu.edu.hk

Abstract

To resolve the discrepancy between the numerical detonation cell size and experimental observations, simulations are conducted with a detailed thermochemical reaction model for a premixed argon-diluted hydrogen-oxygen mixture. Four different scenarios are considered: (i) The whole system is in thermodynamic equilibrium; (ii) the vibrational relaxation is considered and the translational-rotational temperature is used as the dominant temperature of the chemical reactions; (iii) the same non-equilibrium effect as in the second scenario is used along with Park's two-temperature model to account for the effect of vibrational temperature on chemical reaction rates; and (iv) a more physically consistent vibration-chemistry-vibration coupling model is adopted. The simulated detonation cell widths for the first and second scenarios are significantly lower than the experimental measurements, whereas reasonable agreement is observed for the third and fourth scenarios. These results confirm that the involvement of vibrational relaxation in the chemical reactions is an important mechanism in gaseous detonation.

Keywords

Detonation; Cellular structure; Vibrational non-equilibrium; Two-temperature model; CVCV model

Running Head:

Assessment of Vibrational Non-Equilibrium on Detonation

This work has been submitted to Work in Progress Poster (WiPP), 36th International Symposium on Combustion, COEX, Seoul, Korea July 31 - August 5, 2016.

Introduction

Extensive numerical studies have been conducted on the investigation of detonation cellular structures. Detailed chemical reaction models have been adopted in the effort to reveal the physics behind detonations (Hu et al., 2005; Oran et al., 1998). Recent numerical studies have been confronted with the difficulty of matching the simulated cell size with the experimental observations. For a stoichiometric argon-diluted hydrogen-oxygen mixture, the cells are approximately half the measured values, which was attributed to neglect of one of the basic physical processes under supersonic reactive flow, i.e., the vibrational relaxation process, which is neglected when calibrating detailed chemical reaction models (Taylor et al., 2013a).

Within the conditions of detonation, the ratio of ignition delay time over the characteristic timescale for different molecules to reach vibrational equilibrium ranges from 1 to an order of 10^4 according to the estimations of Taylor et al. (2013b). For reference, the ratio of the ignition delay time over the vibrational relation time under the post-shock state of approximately 28 atm and 1540 K for a Chapman-Jouguet detonation in stoichiometric H_2–air at 1 atm and 300 K, assuming that the gas is at thermodynamic equilibrium, and is less than 3 for H_2 and less than 2 for N_2. Within the induction zone after the shock compression, oxygen is not always fully excited vibrationally, and the averaged reaction rate is thus lower than that in the thermal equilibrium assumption (Schott and Kinsey, 1958). Therefore, the important physical mechanism of vibrational non-equilibrium may be important in detailed chemical reaction mechanisms when applied to the simulation of detonation or, more generally, reactive high-speed flows. Unfortunately, no currently available simulation studies have been conducted to quantitatively study the effect on cell size of vibrational relaxation and coupling between vibrational non-equilibrium and chemical reactions.

In this paper, both one-dimensional and two-dimensional numerical simulations of unsteady detonation waves were performed using a recently developed detailed chemical mechanism for high-pressure

combustion of hydrogen. Quantitative comparisons of half-reaction thickness and cell widths from thermodynamic equilibrium cases to thermodynamic non-equilibrium cases are discussed in detail to examine the effect of vibrational non-equilibrium. The interactions between vibrational non-equilibrium and chemical reactions are treated with Park's two-temperature model (1989) and the more recent coupled-vibration-chemistry-vibration (CVCV) model (Knab et al., 1995; Koo et al., 2015; Voelkel et al., 2015).

Physical models and methods

The shock-capturing space-time conservation element and solution element (CE/SE) method, originally proposed by Chang (1995), has been extensively developed and used to handle detonation waves (Shen et al., 2011), hypersonic non-equilibrium flows (Shen et al., 2014), and shock/droplet interactions (Shen et al., 2015a, 2015b; Shen and Wen, 2016). In this study, the second-order CE/SE scheme is used to solve the reactive Euler equations. The stiff source terms are explicitly integrated as ordinary differential equations in an operator-split manner.

We use the recently developed detailed chemical kinetics and thermodynamic data of Burke et al. (2012) for high-pressure hydrogen combustion, which have been endorsed for detonation simulations by other researchers (Taylor et al., 2013a). The NASA Glenn coefficients (McBride et al., 2002) are used to evaluate the chemical equilibrium constants required for the backward reaction rates. The values of specific heat at constant volume are presented by the following equation:

$$C_v = C_{v,\mathrm{tr}} + C_{v,\mathrm{v}}. \tag{1}$$

The total energy per unit volume of a mixture is given by

$$E = \sum_{i=1}^{N\mathrm{s}} \rho_i h_i^f + \sum_{i=1}^{N\mathrm{s}} \rho_i C_{v,\mathrm{tr},i} T_{\mathrm{tr}} + \frac{1}{2}\rho(u^2+v^2) + \sum_{i=\mathrm{molecule}} \rho_i \cdot R_i \cdot \frac{\theta_{\mathrm{v},i}}{\exp(\theta_{\mathrm{v},i}/T_{\mathrm{v}})-1}, \tag{2}$$

in which the last term represents the vibrational energy of the mixture. The characteristic vibrational temperatures of different species are listed in Table 1. Note that the vibrational energy of H_2O_2 is neglected due to its extremely low mass fraction (on the order of 10^{-5} or less). Notably, after shock compression, translational equilibrium is rapidly established, typically in less than 10 molecular collisions. Reaching rotational equilibrium for most small molecules typically requires 10 to 20 molecular collisions, but reaching vibrational equilibrium requires thousands of collisions (Taylor et al., 2013a). Here therefore, we only consider the non-equilibrium effects between vibrational energy and translational-rotational energy. The energy exchange rate is determined by the Landau-Teller relaxation model (Gnoffo et al., 1989) as

$$S_{\text{tr-v}} = \frac{\rho C_{v,\text{v}}}{\tau}(T_{\text{tr}} - T_{\text{v}}). \tag{3}$$

Table 1. Characteristic vibrational temperature of molecules.

Molecule	θ_{v} (K)
H_2	5989
O_2	2250
OH	5140
HO_2	1577, 2059, 5325
H_2O	2297, 5266, 5409

Based on different assumptions, the following four physical models are tested in this paper.

Model (i): Vibrational energy is assumed to be in equilibrium with translational-rotational energy, i.e., $T_{\text{v}} = T_{\text{tr}}$ in Equation 2. The governing equations are the conventional reactive Euler equations.

Model (ii): Considering the vibrational relaxation, an additional transport equation is used to describe the evolution of vibrational energy. The non-equilibrium effect results in different values of T_{tr} and T_{v}. The choice of the dominant temperature of the chemical reaction rate is crucial. In this model, we neglect vibrational-chemical coupling and use T_{tr} as the dominant temperature for all reactions.

Model (iii): Except for the choice of dominant temperature, all other settings remain consistent with model (ii). Considering the vibrational relaxation as in model (ii), Park's two-temperature model (Park, 1989) is used in which the influence of the vibrational temperature on the chemical reaction rates is accounted for. Evidently, the concept of the Arrhenius equation is that two molecules will react when the mutual energy exceeds a certain minimum value. It is reasonable to assume that the vibrational cold mixture is less likely to react than that of the mixture that is fully excited vibrationally. Although it may be ambiguous to ascertain the exact contribution of T_v, an average temperature T_{avg}, defined by the square root of the product of T_{tr} and T_v, is widely used as the dominant temperature of the Arrhenius reaction rate in the community of hypersonic non-equilibrium flows (Park, 1989; Shen et al., 2014). Here, we try to use this concept to investigate the effect of vibrational non-equilibrium on the high-speed reactive flows.

Model (iv): Another approach to examine the effect of vibrational non-equilibrium is the physically consistent CVCV model, which is derived on the assumptions of the T_v-Boltzmann populated vibrational energy mode and truncated harmonic oscillator (Knab et al., 1995). In this model, the chemical reaction rate is modified by an efficiency function, $\varphi(T_{tr}, T_v)$:

$$k\left(T_{tr}, T_v\right) = \varphi\left(T_{tr}, T_v\right) k_{eq}\left(T_{tr}\right). \tag{4}$$

The efficiency function is calculated as:

$$\varphi(T_{tr}, T_v) = \frac{Q(T_{tr}; E_d)}{Q(T_v; E_d)} \cdot \frac{e^{-\alpha E_a / RT} Q(\Gamma; \alpha E_a) + Q(T^0; E_d) - Q(T^0; \alpha E_a)}{e^{-\alpha E_a / RT} Q(-U; \alpha E_a) + Q(T^*; E_d) - Q(T^*; \alpha E_a)}, \tag{5}$$

where $\frac{1}{\Gamma} = \frac{1}{T_v} - \frac{1}{T_{tr}} - \frac{1}{U}, \frac{1}{T^0} = \frac{1}{T_v} - \frac{1}{U}, \frac{1}{T^*} = \frac{1}{T_{tr}} - \frac{1}{U}$. The coefficient α, which determines the fraction of required energy contributed by the translational energy, is selected as 0.8, and $U = E_d / (5R)$ as assessed

in Knab et al. (1995), Koo et al. (2015), and Voelkel et al. (2015). $Q(T;E)=\frac{1-e^{-E/(RT)}}{1-e^{-\theta_v/T}}$ denotes the partition function truncated below energy *E*.

Numerical Results and Discussion

One-dimensional tests

The mixture was composed of stoichiometric hydrogen oxygen diluted with 70% argon at a temperature of 300 K, and the initial pressures were 0.1, 0.2, 0.3, and 0.4 atm, respectively, identical to the initial conditions listed in Taylor et al. (2013a). The meshes were uniformly distributed with Δx = 10 μm. Figure 1 shows the propagating pressure profiles of the mixture at 0.4 atm using model (i). The detonation velocity is 1637 m/s. The detonation is shown as initially overdriven but quickly reaches a self-sustained velocity. Good agreement is observed compared to the Chapman-Jouguet velocity of 1668 m/s. Insignificant differences in the detonation wave speeds were found among the four different models. Figure 2 shows that the calculated half-reaction thickness by using model (ii) is less than that of model (i) only by an extremely small value. However, the half-reaction thickness is significantly increased by using models (iii) or (iv). The distance between the shock front and the position at which H_2 is half consumed is defined as the half-reaction thickness, δ. At 0.1 atm, when the collision frequency is low, the two-temperature model seems to overestimate the vibrational relaxation, as mentioned by Bender et al. (2015) and Panesi et al. (2014). These half-reaction thickness features are further demonstrated in Figure 3.

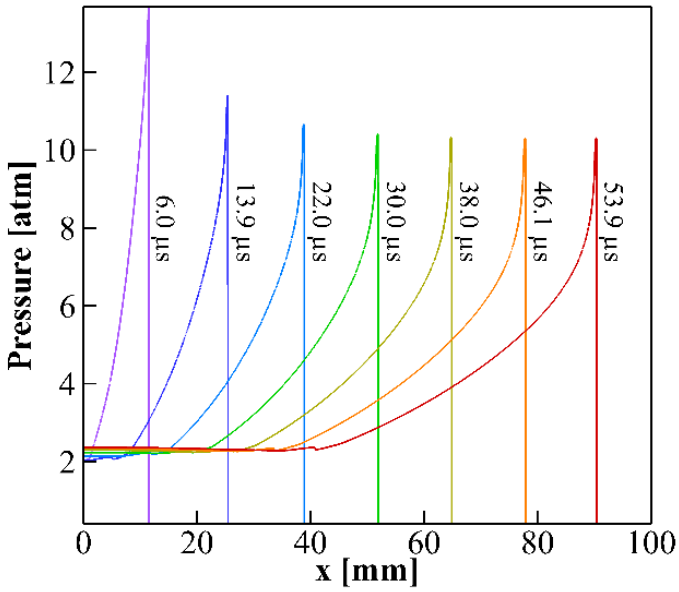

Figure 1. Propagating pressure profiles of model (i) with initial pressure of 0.4 atm and temperature of 300 K.

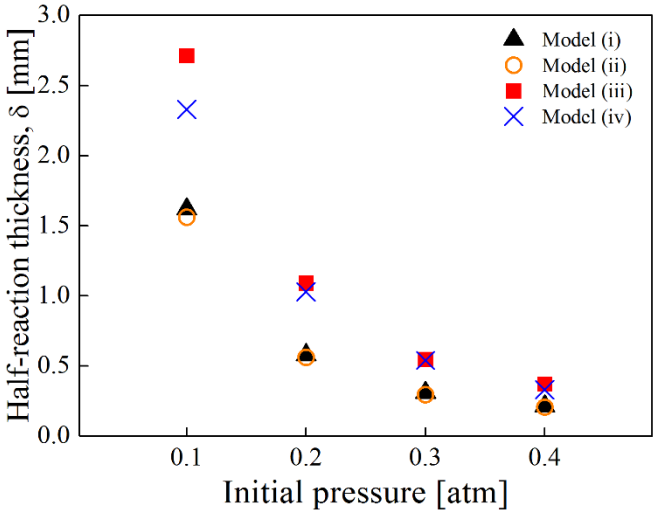

Figure 2. Half-reaction thickness at different initial pressures with initial temperature of 300 K.

Figure 3 illustrates the temperature profiles and H_2 distribution at 0.1 atm and 300 K. As shown in Figure 3a, in the simulation using model (i), the mixture experiences an induction period after being compressed to the post-shock conditions. Because it is thermally perfect, the mixture soon undergoes exothermic reactions that increase the T_{tr}. However, instead of the infinitely fast transfer rate between translational energy and vibrational energy, in the simulation of model (ii), the molecules are almost

vibrational cold behind the shock. The post-shock T_{tr} is even slightly higher than that in model (i). This could be interpreted from Equation 2: the relatively slow vibrational relaxation process, which implies less energy in the vibrational mode and more energy in the translational-rotational mode, prompted T_{tr} to a higher value. However, the minor increase in dominant temperature T_{tr} accelerates the process of the reaction and somewhat narrows the half-reaction thickness. In Figure 3b, however, due to the fact that upon shock compression, T_{tr} undergoes an instantaneous increase, T_v approaches the equilibrium state gradually. As time is required for the molecules to become vibrationally excited before the onset of the severe chemical reaction, the half-reaction thickness in these cases using model (iii) retains an evidently elongated distance (1.67 to 1.76 times that of models (i) and (ii) in these cases). Similar effects can be observed from the case using model (iv) (Figure 3c). According to the semi-empirical correlation of the λ / δ ratio with regard to the conditions of the mixture (Gavrikov et al., 2000), the estimation of one-dimensional detonation δ can roughly describe the effects of the different models on simulating the detonation cell width.

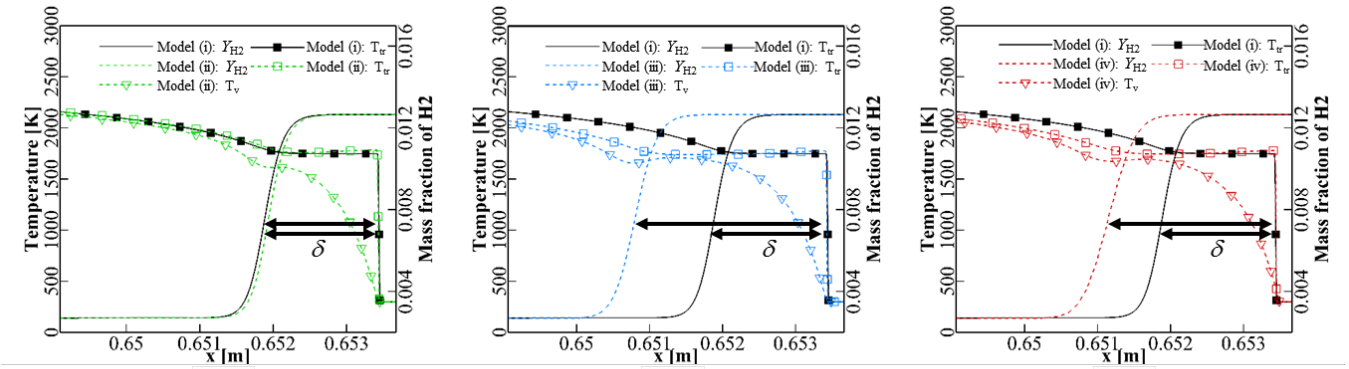

Figure 3. Temperature and H_2 distributions with initial condition of 0.1 atm and 300 K: (a) models (i) and (ii), (b) models (i) and (iii), (c) models (i) and (iv). Note that in models (ii), (iii), and (iv), T_{tr} exhibits overshot behind shock compared to model (i).

Two-dimensional tests

To begin the two-dimensional simulations, the computational domain of the two-dimensional cases was set at 7.76 mm wide, considering the computational efficiency. The mesh spacing was Δh = 10.0 μm, following the conclusion made by Taylor et al. (2013a), in which detonation cells in stoichiometric H_2–O_2 mixtures with 70% Ar dilution initially at 300 K were simulated with detailed chemistry at initial pressures of 0.1, 0.2, 0.3, and 0.4 atm and a finest grid cell spacing of Δh_{min} = 9.766 μm. They showed that further refinement did not change the cell structure or size. In addition, it is suggested that more than 30 grids are required for each detonation cell to emerge in numerical simulations (Gavrikov et al., 2000). In the current research, generally more than 200 cells were assured along each detonation cell widthwise. Using the simulation of Taylor et al. (2013a) as the benchmark, the computational domain was filled with stoichiometric H_2–O_2 diluted with 70% Ar at an initial pressure of 0.4 atm and initial temperature of 300 K. Adiabatic slip wall boundary conditions were adopted at the upper and lower edges of the simulation domain. The mixture was ignited by a small sinusoidal disturbance region with high enthalpy near the left wall. The cell structure performed immediate changes at the very beginning of detonation and continued to adjust to a relatively steady pattern after propagating in the rightward direction for a certain distance. Figure 4 shows the instant contours of model (i) with steady averaged detonation velocity. The fronts of the detonation waves are modestly corrugated.

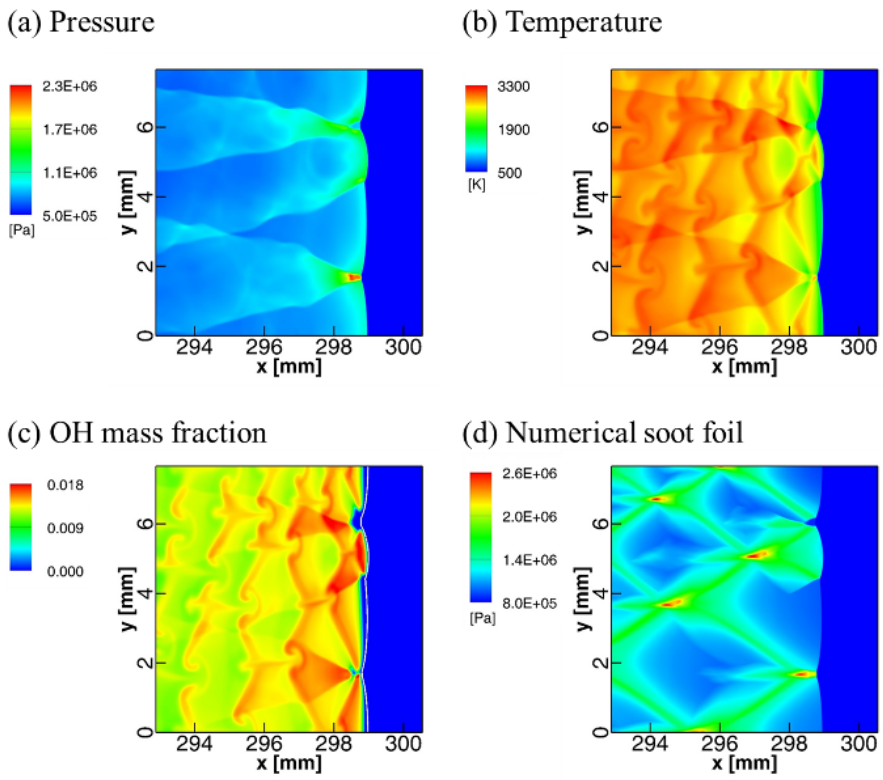

Figure 4. (a) Pressure, (b) temperature, (c) OH field, and (d) numerical soot foil near front of detonation wave using model (i).

It is difficult to measure the half-reaction thickness along the shock front because it varies due to the existence of moving triple points. Nevertheless, it is clear that the values of δ derived by models (iii) and (iv) are generally much wider than those derived by the other two models (Figure 5).

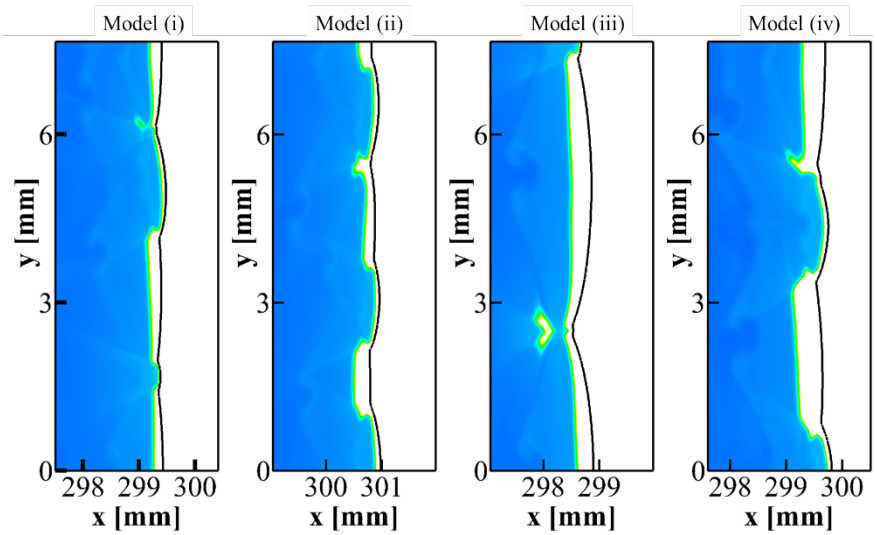

Figure 5. Contour of H_2 as magnified near detonation front; front is indicated by solid black line.

The numerical soot foil was obtained by recording the maximum pressure of the simulation domain as the detonation wave propagated. Snapshots of the numerical soot foil from the four models are shown in Figure 6. In general, the cell size distribution is fairly regular in all four models, which is similar to the findings of Taylor et al. (2013a). The cell structure regularity and averaged cell size in Figure 6a are very similar to those in Figure 6b. Nevertheless, the averaged cell width in Figure 6b is slightly reduced. The cells in Figure 6c and Figure 6d, however, are markedly enlarged. These observations correspond to the expectations from the findings of the one-dimensional calculations in the previous section.

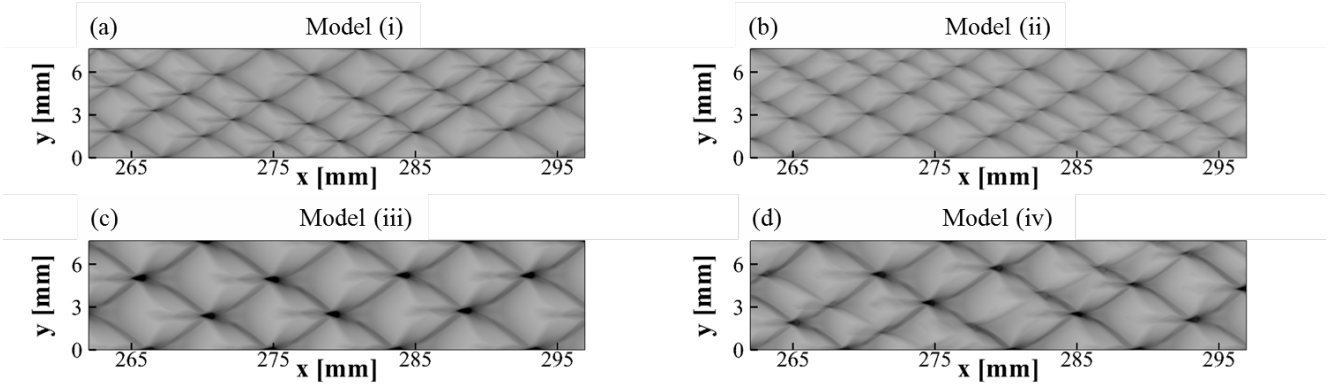

Figure 6. Numerical soot foil using four models.

Figure 7 shows the average width of the detonation cells within the simulation domain. The computed detonation cell widths in the first scenario range from 2.31 to 3.69 mm and are reduced slightly to 1.85 and 3.35 mm in the second scenario. In the third scenario, the computed cell widths dramatically increase to 4.88 to 5.30 mm, whereas they increase to 3.00 to 5.30 mm in the fourth scenario. It is noted that the average cell width of model (ii) is slightly less than that in model (i), whereas the average cell widths in model (iii) and model (iv) are 1.65 times and 1.28 times the average value of those in model (i), respectively. The average cell widths of models (i) and (ii) are consistent with the numerical simulation results of Taylor et al. (2013a) and are significantly lower than the experimental measurement by a factor of approximately 2 for this low-pressure, dilute mixture, despite the use of

different fluid solvers and the same kinetic model. The general agreement of the results suggests that the assumption of thermodynamic equilibrium may not apply over a large portion of the reactive flow in a detonation. Compared to the cell size measured in the experiment (Strehlow and Engel, 1969), the disparity in cell width has been greatly narrowed down to a factor of 1.32 and 1.67 for model (iii) and model (iv), respectively.

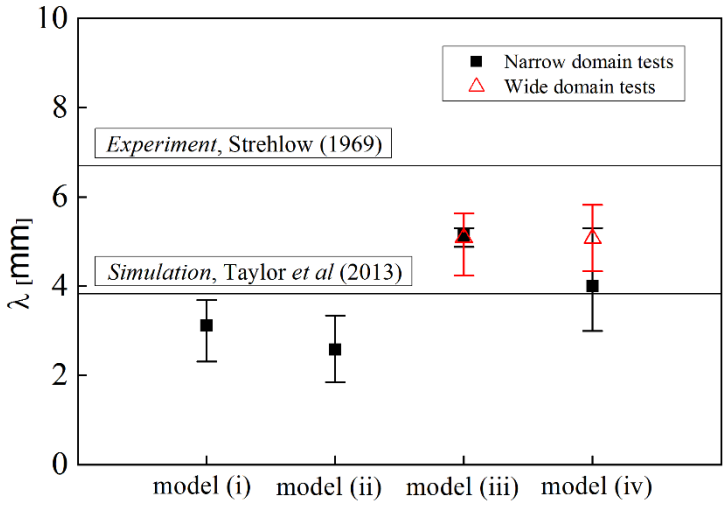

Figure 7. Comparison of detonation cell width obtained in four models.

Because the values of C_v are approximated only by the summation of C_{tr} and C_{vib} (Equation 1), this approach precludes the contribution of the dissociation to the thermodynamic value. This is unavoidable when illustrating the influence of the vibrational relaxation without other distractions. Although this might undoubtedly induce uncertainties into the simulation, such as the lack of accuracy for lateral comparison with previous work in which experimental fitting thermodynamics were adopted, this approach extracts the bias induced by the inconsistency of thermodynamic expression in the governing equations of the different models. Besides the vibrational non-equilibrium, other factors, including mode-locking caused by the limitation of the simulation domain, boundary heat loss and three-dimensional effects, may also considerably affect the detonation cell width. Even with these uncertainties, the apparent distinction between the four models already indicates that vibrational

relaxation can be the possible reason for the difference between previous numerical studies and the present experimental measurements.

Mode-locking tests

Considering possible mode-locking effects when the channel width is close to the detonation cell width, two more simulations using Park's two-temperature model and the CVCV model were conducted with the computational domain width increased from 7.76 to 23.0 mm (3 times larger). Figure 8 presents the numerical soot foils for models (iii) and (iv) using the large simulation domain width. The result indicates that the simulation domain size can affect the cell size to a certain extent. As shown in Figure 7, when a large computational width is used, the average cell size for model (iii) changes insignificantly, whereas that for model (iv) increases from 60% to 77% of the experimental value. Considering the uncertainties in the experiment, reasonable agreement between the simulations of models (iii) and (iv) and the experiment is observed.

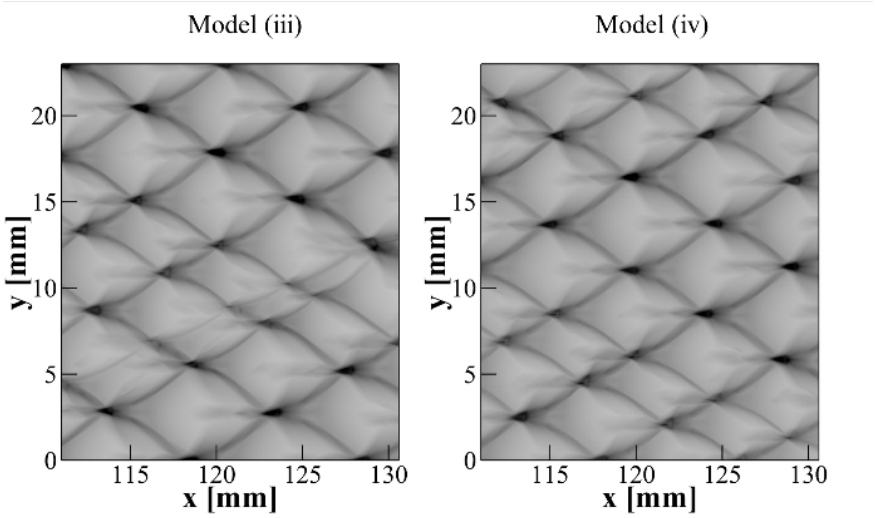

Figure 8. Mode-locking tests for models (iii) and (iv).

Conclusions

The exclusive involvement of vibrational relaxation in the simulation exacerbated the disagreement of detonation cell width with the experimental result if the dominant temperature of the chemical reaction was maintained at T_{tr}. Commensurate with the nature of the assumption that the reaction occurs in extremely combustible conditions, the half-reaction thickness behind the shock could be affected by vibrational non-equilibrium and vibrational relaxation of the gas molecules that occurs on time scales similar to the ignition delay times for the detonations. The vibrational cold state of the molecules might leverage the reaction rates. The reasonable agreement found between the numerically simulated cell width using the geometrically averaged temperature in Park's two-temperature/efficiency function in the CVCV model and the experimental measurement verified the necessity of involving the contribution of the vibrational relaxation process in the evaluation of chemical reaction rates, a process that is presently ignored when calibrating detailed chemical reaction models. Furthermore, this paper reveals the physical mechanism of the effect of vibrational relaxation on the detonation cell size. The contribution from vibrational temperature could vary within a certain range, which will require further careful investigation.

Funding

This research was supported by the opening project of State Key Laboratory of Explosion Science and Technology (Beijing Institute of Technology), numbered KFJJ15-09M. The authors also would like to thank the financial supports by Natural Science Foundation of China under Contract 11372265.

Nomenclature

C_v Specific heat at constant volume

$C_{v,\mathrm{tr}}$ Translational-rotational specific heat at constant volume

$C_{v,\mathrm{v}}$ Vibrational specific heat at constant volume

E_{a} Activation energy

E_{d} Dissociation energy

h^{f} Enthalpy of formation

k_{eq} Reaction rate at vibrational equilibrium condition

M Molecular weight

R Gas constant

$S_{\mathrm{tr\text{-}v}}$ Energy exchange rate between translational-rotational and vibrational energy

T_{tr} Translational-rotational temperature

T_{v} Vibrational temperature

u Velocity along x-direction

v Velocity along y-direction

$Y_{\mathrm{H_2}}$ Mass fraction of H_2

τ Averaged Landau-Teller relaxation time

ρ Density

θ_{v} Characteristic vibrational temperature

λ Detonation cell width

δ Half-reaction thickness

References

Bender, J.D., Valentini, P., Nompelis, I., Paukku, Y., Varga, Z., Truhlar, D.G., Schwartzentruber, T. and Candler, G.V. 2015. An improved potential energy surface and multi-temperature quasiclassical trajectory calculations of N2+ N2 dissociation reactions. *J. Chem. Phys.*, **143(5)**, 054304.

Burke, M.P., Chaos, M., Ju, Y., Dryer, F.L., and Klippenstein, S.J. 2012. Comprehensive H2/O2 kinetic model for high-pressure combustion. *Int. J. Chem. Kinet.*, **44(7)**, 444–474.

Chang, S.C., 1995. The Method of Space-Time Conservation Element and Solution Element–A New Approach for Solving the Navier-Stokes and Euler Equations. *J. Comput. Phys*, **119(2)**, 295-324.

Gavrikov, A.I., Efimenko, A.A., and Dorofeev, S.B. 2000. A Model for Detonation Cell Size Prediction from Chemical Kinetics. *Combust. Flame*, **120(1)**, 19–33.

Gnoffo, P.A., Gupta, R.N., and Shinn, J.L. 1989. Conservation Equations and Physical Models for Hypersonic Air Flows in Thermal and Chemical Nonequilibrium. NASA Langley, Hampton, Virginia, NASA TP-2867.

Hu, X.Y., Zhang, D.L., Khoo, B.C. and Jiang, Z.L. 2005. The structure and evolution of a two-dimensional H_2/O_2/Ar cellular detonation. *Shock Waves*, **14(1-2)**, 37-44.

Knab, O., Frühauf, H.H., and Messerschmid, E.W. 1995. Theory and Validation of the Physically Consistent Coupled Vibration-Chemistry-Vibration Model. *J. Thermophys. Heat Transf.*, **9(2)**, 219-226. (1995).

Koo, H., Raman, V., and Varghese, P. 2015. Direct Numerical Simulation of Supersonic Combustion with Thermal Nonequilibrium. *Proc. Combust. Inst.*, **35**, 2145–2153.

McBride, B.J., Zehe, M.J., and Gordon, S. 2002. NASA Glenn Coefficients for Calculating Thermodynamic Properties of Individual Species, National Aeronautics and Space Administration, Cleveland, Ohio, U.S., NASA report TP-2002-2115 56

Oran, E.S., Weber, J.W., Stefaniw, E.I., Lefebvre, M.H. and Anderson, J.D. 1998. A numerical study of a two-dimensional H_2-O_2-Ar detonation using a detailed chemical reaction model. *Combust. Flame.*, **113(1),** 147-163.

Panesi, M., Munafò, A., Magin, T.E. and Jaffe, R.L. 2014. Nonequilibrium shock-heated nitrogen flows using a rovibrational state-to-state method. *Phys. Rev. E*, **90(1)**, 013009.

Park, C. 1989. Assessment of two-temperature kinetic model for ionizing air. *J. Thermophys. Heat Tr.*, **3(3)** 233-244.

Schott, G.L. and Kinsey, J.L. 1958. Kinetic Studies of Hydroxyl Radicals in Shock Waves. II. Induction Times in the Hydrogen-Oxygen Reaction. *J. Chem. Phys.*, **29(5)**, 1177-1182.

Shen, H., Liu, K.X. and Zhang, D.L. 2011. Three-Dimensional Simulation of Detonation Propagation in a Rectangular Duct By an Improved CE/SE Scheme. *Chin. Phys. Lett.*, **28(12)**, 124705.

Shen, H., Wen, C.Y., and Massimi, H.S. 2014. Application of CE/SE Method to Study Hypersonic Non-equilibrium Flows over Spheres. AIAA 2014-2509.

Shen, H., Wen, C.Y., Liu, K.X., and Zhang, D.L. 2015 (a). Robust High-Order Space-Time Conservative Schemes for Solving Conservation Laws on Hybrid Meshes. *J. Comput. Phys.*, **281**, 375–402.

Shen, H., Wen, C.Y., and Zhang, D.L. 2015 (b). A Characteristic Space-Time Conservation Element and Solution Element Method for Conservation Laws. *J. Comput. Phys.*, **288**, 101-118.

Shen, H., and Wen, C.Y. 2016. A Characteristic Space-Time Conservation Element and Solution Element Method for Conservation Laws II. Multidimensional Extension. *J. Comput. Phys.*, **305**, 775–792.

Strehlow, R.A. and Engel, C.D. 1969. Transverse Waves in Detonations: II. Structure and Spacing in H_2–O_2, C_2H_2–O_2, C_2H_4–O_2, and CH_4–O_2 Systems. *AIAA J.*, **7(3),** 492–496.

Taylor, B.D., Kessler, D.A., Gamezo, V.N., and Oran, E.S. 2013 (a). Numerical Simulations of Hydrogen Detonations with Detailed Chemical Kinetics. *Proc. Combust. Inst.*, **34**, 2009-2016.

Taylor, B.D., Kessler, D.A. and Oran, E.S. 2013 (b). Estimates of Vibrational Nonequilibrium Time Scales in Hydrogen-Air Detonation Waves. Presented at the 24th International Colloquium on the Dynamics of Explosive and Reactive Systems, Taipei, Taiwan, July 28-August 2.

Voelkel, S.J., Raman, V., and Varghese, P. 2015. Non-Equilibrium Reaction Rates in Hydrogen Combustion. Presented at the 25th International Colloquium on the Dynamics of Explosions and Reactive Systems (ICDERS), Leeds, UK, August 2-7.